Bioorganic & Medicinal Chemistry 20 (2012) 5117–5126

Contents lists available at SciVerse ScienceDirect

Bioorganic & Medicinal Chemistry

journal homepage: www.elsevier.com/locate/bmc

Design, synthesis and evaluation of the inhibitory selectivity of novel *trans*-resveratrol analogues on human recombinant CYP1A1, CYP1A2 and CYP1B1

Renata Mikstacka [a,*], Agnes M. Rimando [b], Zbigniew Dutkiewicz [a], Tomasz Stefański [a], Stanisław Sobiak [a]

[a] Department of Chemical Technology of Drugs, Poznan University of Medical Sciences, Grunwaldzka 6, 60-780 Poznan, Poland
[b] United States Department of Agriculture, Agricultural Research Service, Natural Products Utilization Research Unit, PO Box 8048, University, MS 38677, USA

ARTICLE INFO

Article history:
Received 30 March 2012
Revised 2 July 2012
Accepted 6 July 2012
Available online 17 July 2012

Keywords:
P450
CYP1A1
CYP1A2
CYP1B1
trans-Stilbene derivatives
Molecular docking

ABSTRACT

A series of *trans*-stilbene derivatives containing 4′-methylthio substituent were synthesized and evaluated for inhibitory activities on human recombinant cytochrome P450(s): CYP1A1, CYP1A2, and CYP1B1. CYP1A2-related metabolism of stilbene derivatives was estimated by using NADPH oxidation assay. Additionally, for CYP1A2 and CYP1B1 molecular docking analysis was carried out to provide information on enzyme–ligand interactions and putative site of metabolism.

3,4,5-Trimethoxy-4′-methylthio-*trans*-stilbene, an analogue of DMU-212 (3,4,5,4′-tetramethoxy-*trans*-stilbene) was an effective inhibitor of all CYP1 enzymes. On the other hand, 2,3,4-trimethoxy-4′-methylthio-*trans*-stilbene, appeared to be the most selective inhibitor of the isozymes CYP1A1 and CYP1B1, displaying extremely low affinity towards CYP1A2. Molecular modeling suggested that the most probable binding poses of the methylthiostilbene derivatives in CYP1A2 active sites are those with the methylthio substituent directed towards the heme iron. Products of CYP1A2-catalyzed oxidation of 2,4,5-trimethoxy-4′-methylthiostilbene and 3,4,5-trimethoxy-4′-methylthiostilbene were identified as monohydroxylated compounds. Other studied derivatives appeared to be poor substrates of CYP1A2. Structure–activity relationship analysis rendered better understanding of the mechanism of action of xenobiotic-metabolizing enzymes crucial at the early stage of carcinogenesis.

1. Introduction

Chemopreventive, cardioprotective and neuroprotective activities of *trans*-resveratrol (3,4′,5-trihydroxystilbene), the best known natural stilbene derivative, has been documented in numerous studies on animal models.[1] Its therapeutic action in cancer diseases is also under intensive preclinical and clinical studies.[2–4] In the last decade, other natural compounds with stilbene backbone were shown to possess promising activity concerning cancer prevention.[2,5] New stilbene derivatives are designed and synthesized in order to find resveratrol analogues with cancer chemopreventive and/or therapeutic activities superior to that of the parent compound. The compounds are examined with respect to different targets such as estrogen receptors,[6] COX 1/2,[7] signal transduction pathways,[8,9] cell proliferation,[10] and inhibitory activity towards cytochromes P450 (CYPs). The studies are focused on structure–activity relationship in order to identify structural determinants responsible for beneficial activities of stilbene derivatives. Other investigations are aimed to find resveratrol analogues that demonstrate better bioavailability than the parent compound that undergoes fast biotransformation to glucuronides and sulfates.[11] Methoxylation of hydroxyl groups is supposed to prevent polyphenol metabolism and enhance stilbene bioactivity.[12,13]

Cytochrome P450 family 1 includes xenobiotic-metabolizing enzymes: CYP1A1, CYP1A2 and CYP1B1 that catalyze the activation of environmental procarcinogens such as polycyclic aromatic hydrocarbons, aromatic and heterocyclic amines to carcinogenic forms. Additionally, CYP1B1 metabolizes 17β-estradiol to 4-hydroxyestradiol that is oxidized by peroxidase to estradiol-3,4-quinone, and forms a quinone-DNA adducts responsible for estrogen-related carcinogenesis.[14] For these reasons, there is a demand for inhibitors that demonstrate high selectivity toward specific forms of cytochrome 450; namely, CYP1A1 and CYP1B1 for blocking CYP-related carcinogenesis. CYP1A2 metabolizes numerous xenobiotics including drugs such as cafeine, theophylline, methadone, verapamil, propranolol, warfarin, and tamoxifen. Not much is known about CYP1A2; hence its properties, the structure of its active site and substrate specificity need thorough investigation. All members of CYP1A family are expressed in extrahepatic tissues; however, CYP1A2 is the only constitutive form of liver enzyme. In humans CYP1B1 is overexpressed in tumor cells, and this has important

* Corresponding author. Tel./fax: +48 618 546 625.
E-mail address: rmikstac@ump.edu.pl (R. Mikstacka).

0968-0896/$ - see front matter © 2012 Elsevier Ltd. All rights reserved.
http://dx.doi.org/10.1016/j.bmc.2012.07.012

implications for tumor development and progression. Thus, regulators of the expression and catalytic activity of Family 1 cytochromes are suggested to play an important role in cancer chemoprevention mainly at the early stage of tumorigenesis; specifically, development of anticancer prodrugs specifically activated by CYP1B1 is a promising strategy in cancer chemotherapy.[15] Moreover, it was discovered recently that CYP1B1 generates reactive oxygen species (ROS) leading to hypertension,[16] therefore, CYP1B1 inhibitors might be of therapeutic importance in cardiovascular diseases.

The diverse activities of resveratrol include moderate inhibition of CYP1A1 and CYP1B1, and rather weak inactivation of CYP1A2.[17] Natural resveratrol methyl ethers appeared to be more specific and potent inhibitors of cytochromes P450 (CYP) Family 1 in comparison to the parent compound.[18–20] Many synthetic methoxy stilbene derivatives were tested for inhibitory activity toward CYP1 isozymes. 3,5,2′,4′-Tetramethoxystilbene and 2,6,2′,4′-tetramethoxystilbene appeared to be potent and specific inhibitors of CYP1B1;[21,22] while natural resveratrol analogue, rhapontigenin (3,5,3′-trihydroxy-4′-methoxystilbene) was found to inhibit selectively CYP1A1.[23] Results from our previous study revealed that some of stilbene derivatives with methylthio substituent are selective and potent inhibitors of CYP1 enzymes.[24] Among the series of compounds investigated earlier, 2-methoxy-4′-methylthiostilbene and 3-methoxy-4′-methylthiostilbene were the most potent competitive inhibitors of CYP1A1 and CYP1B1 activities.[24] Methylthiostilbene derivatives merit attention in view of the fact that substitution of the 4′-oxygen atom with the less electronegative sulfur atom reduces toxicity to HEK 293 cells, and as was observed by Yang et al.[25] enhances the ability of the compound to activate human Sirtuin-1.

In this study we extended our studies of 4′-methylthiostilbene derivatives and synthesized seven new compounds differing in the substitution pattern and performed computational docking of synthesized compounds in CYP1A2 and CYP1B1 active sites. Computational modeling and docking procedures provide additional information on mechanism of enzyme inhibition at the molecular level; make analysis of binding orientations of inhibitors to enzyme active sites possible and allow prediction of putative sites of metabolism.[26] These procedures are helpful in structure–activity relationship analysis and as such, are employed for verification of hypothesis based on experimental results. Moreover, in silico tools are useful in the design of more efficient and selective synthetic inhibitors of enzymes. Models of cytochrome P450 enzymes as key enzymes metabolizing exogenous and endogenous substrates have been created and well characterized.[27] Molecular docking of different CYP1 substrates has been reported, for example, rutaecarpine derivatives,[28] 7-alkoxylresorufins,[29] coumarins,[30] and methoxyflavonoids;[31] however, computational analysis of stilbenes as substrates of CYP1 enzymes is still lacking.

In our present study, a series of 4′-methylthiostilbenes differing in methoxy groups patterns in ring A (Table 1) were synthesized and examined for their inhibitory effects on activities of human recombinant CYPs: CYP1A1, CYP1A2 and CYP1B1. In order to elucidate the inhibition selectivity of some 4′-methylthiostilbenes, which exerted potent and selective inhibition of CYP1B1, molecular docking approach was used. We found two 4′-methylthiostilbene derivatives as substrates of CYP1A2 and identified the products of their metabolism. Additionally, on the basis of CYP1A2 computational docking, the site of metabolism was predicted and the results of virtual screening were compared with experimental data. The specific interactions that govern orientation of an inhibitor/substrate in the enzyme active site are discussed.

2. Results and discussion

2.1. Chemistry

The synthesis of compounds is outlined in Scheme 1. The key synthetic step for the construction of these compounds involves the generation of phosphonate ester **2** (diethyl-4-meth-

Table 1
Summary of IC_{50} values for EROD inhibition by a series of 4′-methythiolstilbene derivatives

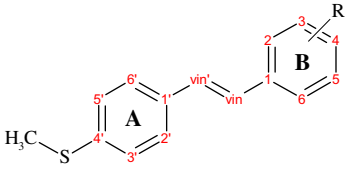

	IC_{50} (μM)			Ratio		NADPH oxidized[b]
	CYP1A1	CYP1A2	CYP1B1	CYP1A2/CYP1A1	CYP1A2/CYP1B1	
Monomethoxy-4′-methylthiostilbenes						
2-M-4′-MTS[a]	1.0	7.5	0.3	7.5	25.0	<0.3
3-M-4′-MTS[a]	1.1	11.5	0.5	10.5	23.0	<0.3
4-M-4′-MTS[a]	28.0	23.0	5.5	0.8	4.2	<0.3
Dimethoxy-4′-methylthiostilbenes						
2,3-DiM-4′-MTS[a]	1.8	22.0	1.1	12.2	20.0	<0.3
2,4-DiM-4′-MTS (**S1**)	2.4	8.1	2.0	3.4	4.1	<0.3
2,5-DiM-4′-MTS (**S2**)	3.8	39.5	1.1	10.4	35.9	<0.3
3,5-DiM-4′-MTS[a]	1.4	5.0	1.5	3.6	3.3	<0.3
Trimethoxy-4′-methylthiostilbenes						
2,3,4-TriM-4′-MTS (**S3**)	0.9	>50	1.0	>55.5	>50	<0.6
2,4,5-TriM-4′-MTS (**S4**)	0.8	15.0	0.9	18.7	16.7	2.91
2,4,6-TriM-4′-MTS (**S5**)	0.4	6.5	0.5	16.3	17.0	<0.3
3,4,5-TriM-4′-MTS (**S6**)	3.6	7.0	2.6	1.9	2.7	2.22
2-Chloro-4′-MTS (**S7**)	1.0	14.5	0.3	14.5	48.33	Not determined

Each IC_{50} value was calculated by plotting the inhibition of EROD activity against the inhibitor concentration. The determination was performed in three parallel experiments. The coefficient of variation did not exceed 15%.

[a] Compounds studied earlier (Mikstacka et al., 2008). M = methoxy; MTS = methylthiosilbene.

[b] Values are in M/pmol CYP1A2/min. Stilbenes were dissolved in DMSO; the amount of DMSO did not exceed 0.5%. The concentration of stilbenes in reaction mixture was 10 μM. The level of NADPH oxidation when only DMSO as a vehicle was added was equal 0.3 μM/pmol CYP1A2/min.

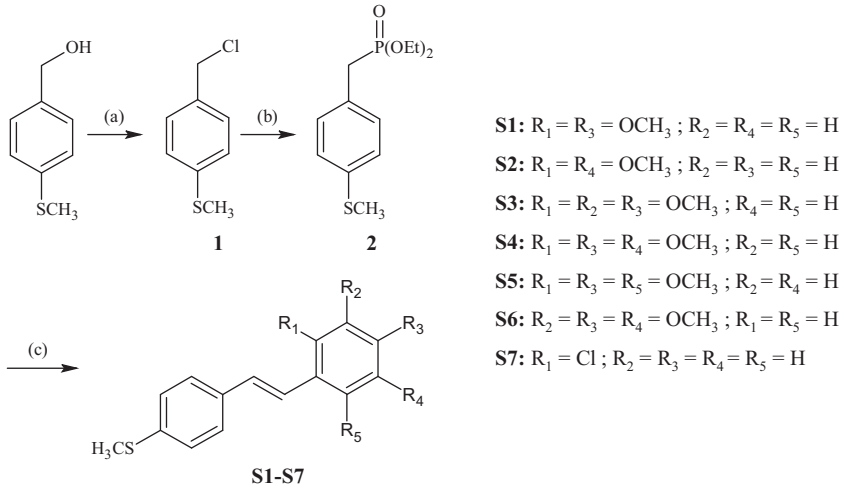

Scheme 1. General synthetic route for the synthesis of the *trans*-methylthiostilbene analogues (**S1**–**S7**). Reagents and conditions: (a) $SOCl_2$, toluene, 0.5 h, room temp, 84%; (b) $P(OEt)_3$, 130 °C, 2 h, 80%; (c) (R_1–R_5)PhCHO, NaH, DMF, 0 °C to room temp, 2 h, 48–75%.

ylthiobenzylphosphonate) as an intermediate. This was prepared from commercially available 4-methylthiobenzyl alcohol in two steps. First, 4-methylthiobenzyl alcohol was converted to the chloride **1** using $SOCl_2$ in toluene at room temperature. Then, through the Michaelis–Arbuzov reaction of **1** with triethylphosphite at 130 °C the corresponding phosphonate ester **2** was obtained. *trans*-methylthiostilbene analogues were prepared by Wittig–Horner reaction of **2** with the commercially available benzaldehydes in DMF using sodium hydride as a base. Under these reaction conditions *trans*-isomers were obtained exclusively. Geometries of these compounds were confirmed by their characteristic ^1H NMR coupling constants for the olefinic protons of about 16–16.5 Hz.

Intermediates were characterized by NMR spectroscopy. Final products were characterized by NMR, and mass spectrum, which were in full accordance with depicted structures. One of the studied compounds, **S6** was reported earlier by Cushman et al.[8]

2.2. Inhibitory effect on CYP1A1, CYP1A2 and CYP1B1 activities

The inhibitory activities of synthesized 4′-methylthiostilbene (4′-MTS) analogues 2,4-dimethoxy-4′-MTS (**S1**), 2,5-dimethoxy-4′-MTS (**S2**), 2,3,4-trimethoxy-4′-MTS (**S3**), 2,4,5-trimethoxy-4′-MTS (**S4**), 2,4,6-trimethoxy-4′-MTS (**S5**) 3,4,5-trimethoxy-4′-MTS (**S6**), and 2-chloro-4′-MTS (**S7**) on human recombinant cytochrome P450(s) CYP1A1, CYP1A2 and CYP1B1 were evaluated and compared with those of 4′-methylthiostilbenes previously investigated.[24] IC_{50} values for the series of polymethoxy 4′-methylthiostilbenes are summarized in Table 1. In the CYP1B1 inhibition assay, **S7** and two 4′-MTS analogues studied earlier, that is, 2-methoxy-4′-MTS and 3-methoxy-4′-MTS, were the potent inhibitors with IC_{50} values of 0.3, 0.5 and 0.3 μM, respectively. Interestingly, substitution of 2-methoxy group with chlorine atom did not change the inhibitory activity of 4′-MTS derivative toward CYP1A1 and CYP1B1. However, the substituent at the position 2 seems to play a crucial role in CYP1B1 inhibition, which is in agreement with earlier reports.[21,22]

All the stilbenes studied appeared to be strong or moderate inhibitors of CYP1B1 with IC_{50} <2.6 μM. 2,3,4-Trimethoxy-4′-MTS (**S3**) was found to be the most selective inhibitor of the enzymes CYP1A1 and CYP1B1, and exerted very low affinity to CYP1A2. Experimental data suggested that there was not a single structural determinant for selective inhibition of the 4′-methylthiostilbenes; rather, the pattern of substitution on ring A of the stilbene scaffold determined the inhibitory properties. For example, among the dimethoxy derivatives, those having the substituents in *meta* position to each other seem to have better affinity to the CYP1A2 active site (thus lower IC_{50} values for **S1** and 3,5-dimethoxy-4′-MTS, see Table 1); however, to confirm that observation a bigger series of compounds should be tested.

All stilbene derivatives used in this study showed moderate to weak inhibitory activity towards CYP1A2 in comparison with CYP1A1 and CYP1B1. However, basing on the experimental inhibition data it is noticeable that CYP1A2 is the most susceptible to variations in the pattern of methoxy substituents. The 4′-methylthiostilbenes may be divided into two distinct groups: relatively good (IC_{50} <10 μM) and very weak (IC_{50} >10 μM) inhibitors. Interestingly, the motif 3,4,5-trimethoxy did not diminish the affinity of this trimethoxy derivative to CYP1A2, while it influenced significantly the inhibitory potency towards CYP1A1 and CYP1B1. It may be concluded that analogues where the substituents in ring B are arranged in such a way where half of ring B (when an imaginary line is drawn from C1 to C4) mirrors the other half of the ring provide relatively strong inhibition of CYP1A2.

S3, **S4**, and **S5** appeared to be the most potent inhibitors of CYP1A1 (IC_{50} <1 μM). Comparing the potency of test compounds towards different CYP1 isoforms it may be concluded that IC_{50} values determined for CYP1A1 and CYP1B1 correlate with each other with few exceptions of monomethoxy-4′-methylthiostilbenes and **S2**.

2.3. Metabolism studies

To examine whether the stilbene derivatives were metabolized in CYP1A2-catalyzed reaction, NADPH oxidation in the presence of CYP1A2 was measured spectrophotometrically. Significant CYP1A2-related metabolism was observed only for **S6** and **S4** (Table 1). The effect of NADPH oxidation was observed at lower stilbene concentrations (⩽10 μM); at higher concentrations NADPH was oxidized less effectively (data not shown). It appeared that at higher concentrations inhibitory effect of **S6** and **S4** on CYP1A2 activity might be prevailing. However these speculations need to be elucidated by further experimental explorations.

The products from CYP1A2-catalyzed metabolism of **S6** and **S4** were analyzed by GC–MS, which revealed monohydroxylated metabolites. The total ion chromatograms (TIC) of pure samples of **S6** and **S4** showed single peaks (retention times 11.58 min and 11.92; Figs. 1A and 2A, respectively) and molecular ion peaks of 316 amu (Figs. 1B and 2B, respectively). Upon reaction with CYP1A2, the **S6** reaction mixture showed a peak (Fig. 1C1 and

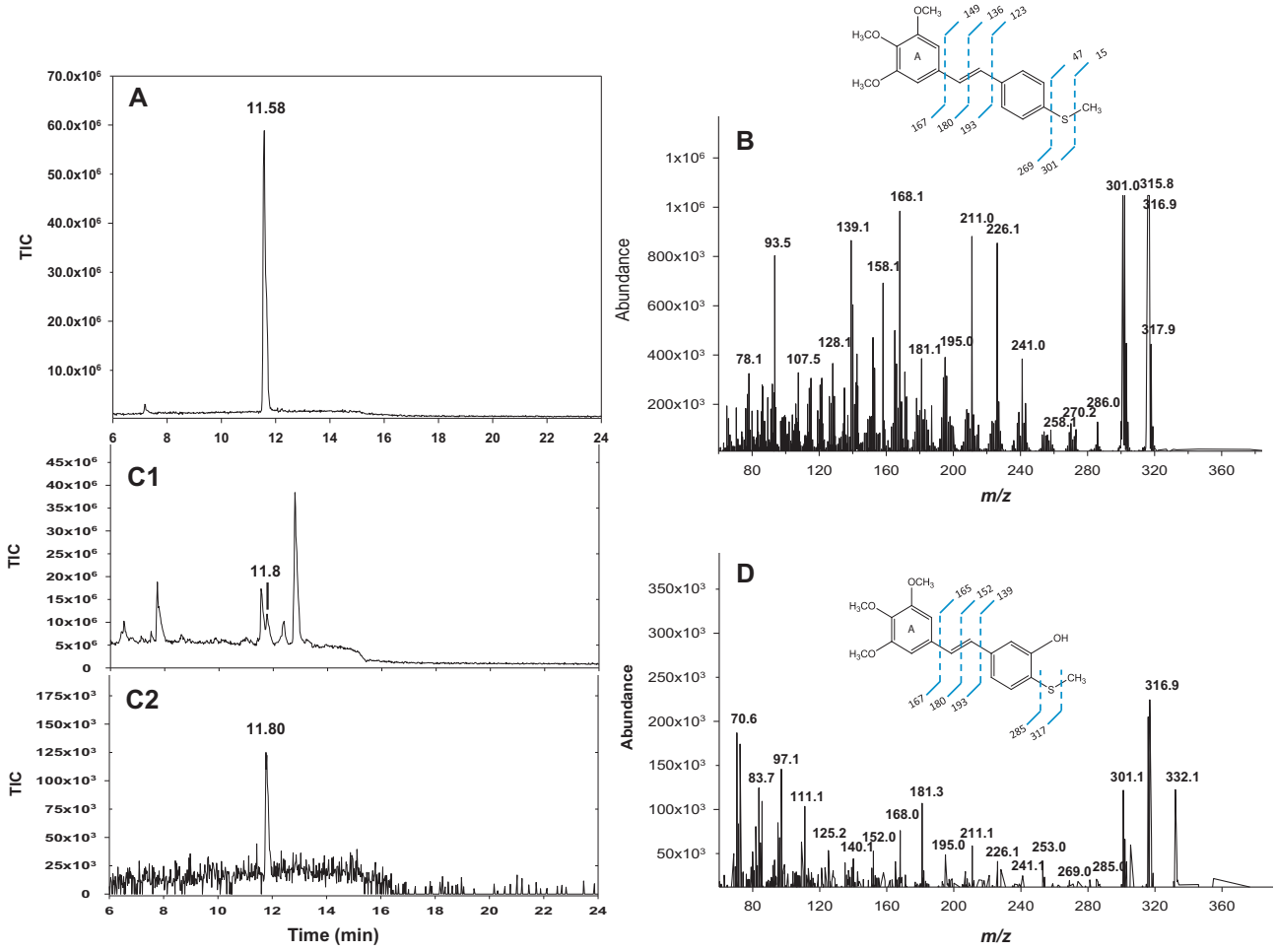

Figure 1. GC–MS analysis of 3,4,5-trimethoxy-4′-thiomethyl-*trans*-stilbene (**S6**). (A) Total ion chromatogram (TIC) of pure **S6**, retention time = 11.58 min. (B) Mass spectrum of **S6** showing molecular ion *m*/*z* 316 and characteristic fragmentation. (C1) TIC of the ethyl acetate extract of the CYP1A2 and **S6** reaction mixture, showing a single peak when mass-defined at *m*/*z* 332 (C2) indicative of addition of one hydroxyl group. (D) Mass spectrum of peak in panel C2 at 11.80 min showing molecular ion at *m*/*z* 332 and characteristic fragmentations.

C2) with mass 332 amu (Fig. 1D). Similarly, reaction of CYP1A2 with **S4** showed a peak (Fig. 2C1 and C2) with mass 332 amu (Fig. 2D). Mass spectral data indicated that hydroxylation occurred on ring B evident from the presence of fragmentation peaks *m*/*z* 140 and 152, as well as intact ring A fragment peaks at *m*/*z* 168, 181, and 195 for **S6** (Fig. 1D, see also inset). Similarly, for **S4** hydroxylation on ring B was evident from the presence of fragmentation peaks *m*/*z* 139, 152 and 165, as well as intact ring A fragment peaks at *m*/*z* 181 and 195 (Fig. 2D, see also inset). Considering that 3,5,3′,4′-tetrahydroxystilbene (piceatannol) is a product of resveratrol 3′-hydroxylation catalyzed by CYP1A2,[32] it is most probable is that the hydroxy group was introduced at the position 3′ of B ring. In our experiments, the structure of identified products confirms the orientation of stilbenes in the CYP1A2 active site cavity predicted by means of molecular docking. Moreover, these metabolites might be inhibitors of CYP1A2 activity. We can only speculate from the molecular modeling, that it might be difficult for such bulky molecules to leave the enzyme cavity through an entrance canal or that the binding of the hydroxy metabolites to the CYP1A2 active site is irreversible.

2.4. Molecular docking

Molecular docking for the series of 4′-MTS derivatives included in this study into the active sites of CYP1A2[33] and CYP1B1[34] was conducted in order to elucidate the selectivity of CYP1 inhibition by stilbenes differing in substitution pattern in the A ring. We explored the possible binding modes for the compounds that differed in inhibitory potency toward CYP1A2 and CYP1B1. Basing on the evalution of molecular docking programs[35,36] we chose LigandFit as the appropriate and we validated its performance with 7,8-benzoflavone and 7-ethoxyresorufin as ligands. With the use of LigandFit docking procedure, we analyzed orientations of the test molecules in the enzyme active sites, to choose those that are the most probable.

Among all poses of the studied compounds in the active site cavity of CYP1A2 the most frequent occurring were the poses with B ring localized close to the heme. Docking procedure found some exceptions when A ring was directed towards the heme: one of two poses found for 2-methoxy-4′-MTS and two poses found for **S7**. Ligands in the enzyme active site were stabilized by a single π–π stacking interaction between Phe226 and ring B and A in 'reversed' poses (Fig. 3A). Some exceptions were observed for 3-methoxy-4′-MTS when two π–π stacking interactions of Phe226 with A and B ring and for **S2** when two π–π stacking interactions of Phe226 occurred with A and B ring and additionally a π–π stacking interaction of Phe260 with A ring was found. However, these exceptional orientations seem to be less effective because of increased distances of ligand to the heme. More importantly, for **S2**, **S4**, **S5**, **and S6**, but not **S3**, docking procedure has found poses

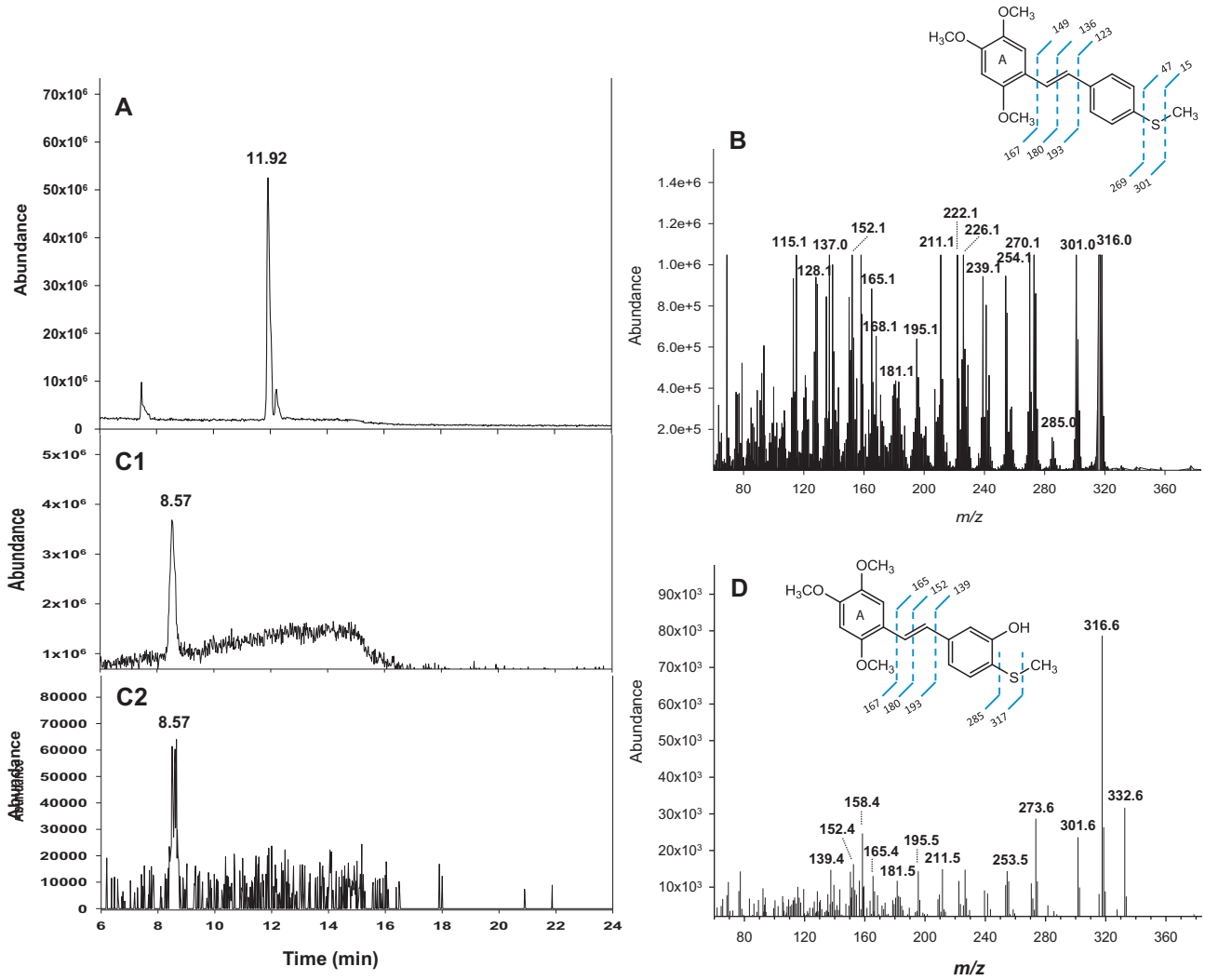

Figure 2. GC–MS analysis of 2,4,5-trimethoxy-4′-thiomethyl-*trans*-stilbene (**S4**). (A) Total ion chromatogram (TIC) of pure **S4**, retention time = 11.92 min. (B) Mass spectrum of **S4** showing molecular ion *m*/*z* 316 and characteristic fragmentation. (C1) TIC of the ethyl acetate extract of the CYP1A2 and **S4** reaction mixture, showing a single peak when mass-defined at *m*/*z* 332 (C2) indicative of addition of one hydroxyl group. (D) Mass spectrum of peak in panel C2 at 8.58 min showing molecular ion at *m*/*z* 332 and characteristic fragmentations.

stabilized by two π–π stacking interactions of ring A with Phe226 and Phe260. Docking of **S3** in CYP1A2 cavity resulted in three distinct poses; however in one of them, the lowest in DockScore ranking, a π–π stacking interaction was not found. Moreover, the best pose of **S3** was classified at the lowest position among the best poses of the studied series of compounds, while its strain energy achieved the highest value (103.09 kcal/mol; for more data see Supplementary data); these data support weak inhibitory activity demonstrated experimentally. The ideal poses for metabolized **S4** and **S6** possessed two π–π interaction within Phe260 and Phe226 and additionally, for **S6** hydrophobic interaction with Gly316 for ring A has occurred (Fig. 4). The orientations let the molecules be close to the heme and promote the oxidation of ring B in the vicinity of 4′-methylthio group. The distances between Fe atom and C atoms in 3′ and 5′ positions for **S4** were 5.44 and 4.46 Å, respectively. Corresponding values for **S6** were 5.37 and 4.38 Å (the data concerning the other test stilbenes are in Supplementary data). Interestingly, for **S2** and **S5** two π–π interactions within Phe226, Phe260 and the ring A did not bring the molecules closer to the heme what was in agreement with poor oxidation of these compounds; contrary, these π–π interactions caused the significant increase of distances of C atoms in 3′ and 5′ positions to Fe atom.

Identified by GC–MS, oxidized products of **S6** and **S4** provided additional evidence that the most effective poses are those when the ring B is directed towards the heme (Fig. 4). The stilbenes that are not metabolized by CYP1A2 probably inhibit *O*-deethylation of 7-ethoxyresorufin by binding to a site that only partially involves the catalytic site. Binding to the regulatory sites that causes a change in the cytochrome structure and shape may be taken into account as a mechanism of enzyme inhibition. The other explanation for the lack of metabolism observed for several derivatives is that the molecules did not sufficiently come close to the heme. For effective enzymatic reaction, the distance of a substrate to the heme iron should not exceed 6 Å.[37] However, specific interactions between an inhibitor and amino acid residues in the enzyme cavity govern orientation of a molecule in the active site. For example, methoxy substituents on the A ring may influence better fit of the molecule to the binding site cavity by hydrophobic interactions or hydrogen bonding. Schematic representation of ligand interactions with amino acids residues visualizes the predominant role of hydrophobic interactions (Fig. 3A). Moreover, these interactions may produce an effect of shortening of the distance between B ring and the iron. It is worth mentioning that for the metabolized derivatives **S4** and **S6** docked in CYP1A2 binding site, the distances be-

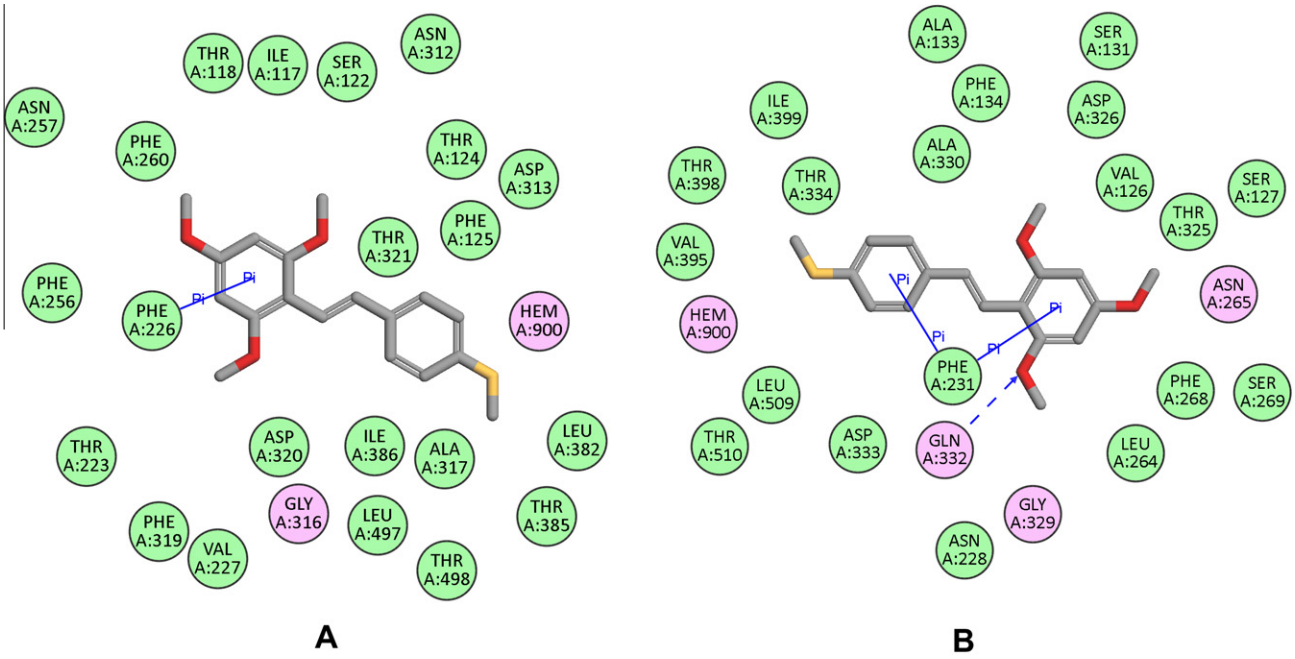

Figure 3. The amino acid residues surrounding 2,4,6-trimethoxy-4′-methylthio-*trans*-stilbene (**S5**) in (A) CYP1A2 and (B) CYP1B1 binding sites. Residues involved in van der Waals and polar interactions are colored in green and magenta, respectively. Solid blue lines represent π–π interactions and dashed blue lines represent hydrogen bonds.

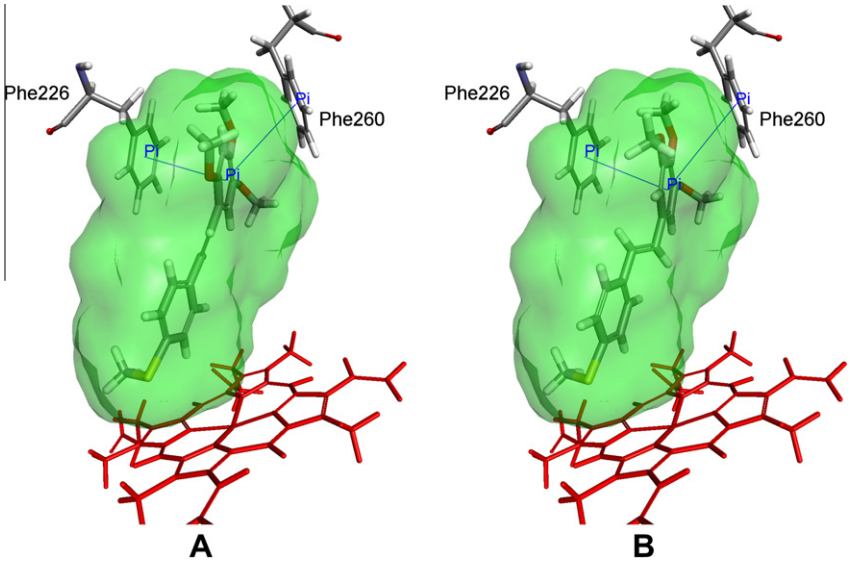

Figure 4. Human CYP1A2 active site in complex with (A) 2,4,5-trimethoxy-4′-methylthio-*trans*-stilbene (**S4**) and (B) 3,4,5-trimethoxy-4′-methylthio-*trans*-stilbene (**S6**). Solid blue lines represent π–π interactions. Heme is represented as a stick model in red.

tween Fe atom and C atoms in 3′ and 5′ positions were shorter than 5.5 and 4.5 Å, respectively.

Analysis of the three-dimensional structures of polymethoxystilbenes showed that in in **S3**, both 2- and 3-methyl groups are displaced from the aromatic ring A plane and are on opposite sides of this plane. However distortion of methyl group is not considered a decisive conformational change, it seems to us that in case of bulky trimethoxy derivative it may be a reason for a very low affinity of this compound to CYP1A2 active site, which is described as narrow and suitable for rather flat ligand molecules. Furthermore, fitting of this trimethoxystilbene to CYP1A2 active site leads to the significant increase of strain energy and seems not to be energetically favorable. Figure 5 illustrates the best poses of **S3** in CYP1A2 and CYP1B1 and demonstrates the conformational changes of the ligand in the enzyme cavity.

In the active site of CYP1B1 the orientation of 4′-MTS derivatives was the same as in CYP1A2 with B ring directed towards the heme with some exceptions: 3 of 4 poses found by LigandFit for 4-methoxy-4′-MTS and 1 of 4 poses found for 2,3-dimethoxy-4′-MTS were reversed, with A ring oriented towards the heme. However, the 4′-MTS derivatives exerted much more potent inhibitory activity towards CYP1B1 in comparison to CYP1A2. Higher affinity of 4′-MTS to CYP1B1 than CYP1A2 is well supported by DockScore function values which are significantly higher in case of CYP1B1 (see Supplementary Table S1). This function was determined for the most selective CYP1B1 inhibitor, **S3**, to be 7-fold

higher as compared with CYP1A2. For the best pose of this trimethoxy derivative strain energy decreased from 103.09 in CYP1A2 binding site to 40.7 kcal/mol in CYP1B1 binding site.

For CYP1B1 two π–π stacking interactions between Phe231 and A and B rings of studied stilbenes were found (Fig. 3B) with some minor exceptions when only one π–π stacking interaction occurred. Additionally, for some of ligands docked in the CYP1B1 cavity hydrogen bonds were found. For monitoring hydrogen bonds the default value of 2.5 Å as a distance criterion was used. The ability of hydrogen bond formation by Gln332 in the CYP1B1 active site may influence high inhibitory activity of stilbenes substituted on position 2.[21,22] An exceptional behavior of **S4** is worth presenting. This stilbene was oriented by docking procedure with 5-methoxy group pointed toward Gln332 residue and involved in hydrogen bonding that made the molecule come closer to the heme; as a result, a π–π stacking interaction of B ring was impossible to occur.

Summarizing, the docking study has shown that specific amino acid residues for each CYP1 play an important role in the interactions of the 4′-MTS derivatives in the enzyme pocket. The critical residues identified as participating in π–π stacking interactions are Phe226 and Phe260 for CYP1A2, and Phe231 for CYP1B1. However, Phe231 in CYP1B1 active site interacts with the both aromatic rings of the stilbenes, while in the case of CYP1A2 the most frequent interaction is only with one of the rings, namely A ring. Additionally, in the case of CYP1B1 Gln332 takes part in hydrogen bonding of methoxy substituents. Comparing the influence of a series of 4′-MTS derivatives on CYP1B1 activity the highest inhibitory effect was observed for 2-methoxy- and 3-methoxy-4′-MTS analogues; these compounds inhibited CYP1B1 activity in a competitive manner with K_i values 0.04 and 0.03 μM, respectively.[24] However, all stilbenes tested were relatively potent CYP1B1 inhibitors, it may be speculated that in the case of other members of this series, additional methoxy groups did not help in achieving better affinity to CYP1B1 active site. On the other hand, polymethoxylated A ring influences significantly the affinity of stilbene derivatives towards CYP1A2 and in this way improves the selectivity of CYP1 inhibition.

3. Conclusions

A series of di- and tri-methoxy-4′-MTS derivatives were synthesized using efficient methods. The compounds were evaluated for their inhibitory potency towards CYP1A1, CYP1A2 and CYP1B1 activities. 2,3,4-Trimethoxy-4′-MTS, **S3**, was the most selective inhibitor of CYP1A1 and CYP1B1, while displaying extremely low affinity toward CYP1A2, which was explained by in silico studies. Substitution of 2-methoxy group with chlorine atom did not change the inhibitory activity of 4′-MTS derivative toward CYP1A1 and CYP1B1. Molecular modeling studies revealed several π–π stacking interactions for CYP1A2 and CYP1B1 active site; additionally for CYP1B1 hydrogen bonds with Gln332 were found for 2-MTS, **S2**, **S4**, **S5**, and **S6**. The residues Phe226 and Phe260 for CYP1A2, and Phe231 for CYP1B1 were involved in the π–π stacking interactions with aromatic rings of polymethoxy-stilbene derivatives. Whatever interaction found for the least active analogue **S3** in CYP1A2 cavity, together with DockScore function, characterized this compound with very low value. Conversely, in CYP1B1 active site the orientation of this trimethoxy derivative was stabilized by π–π stacking interaction with Phe231 and its strain energy was 2.5-fold diminished.

CYP1A2 effectively metabolized **S4** and **S6** to products with hydroxyl group substituted on B ring as identified by means of GC–MS. Other stilbene derivatives studied were not metabolized by CYP1A2; however, CYP1A2-catalyzed *O*-deethylation of 7-ethoxyresorufin was inhibited in their presence. In this case, the stilbenes probably bind to a site other than the catalytic site of enzyme. Molecular docking studies suggested the preferred orientation of the 4′-methylthiostilbene derivatives with the thiomethyl substituent on B ring directed towards the iron heme. The stilbene molecules might also be oriented with the A ring towards the heme; however, that position was not energetically favorable. In fact, the products hydroxylated at A ring were not found.

Summarizing, study of the inhibitory activity of stilbene derivatives enriched our knowledge of CYPs properties and mechanism of CYP-related catalysis. Computational screening of compounds with the use of enzyme model supported experimental data, and

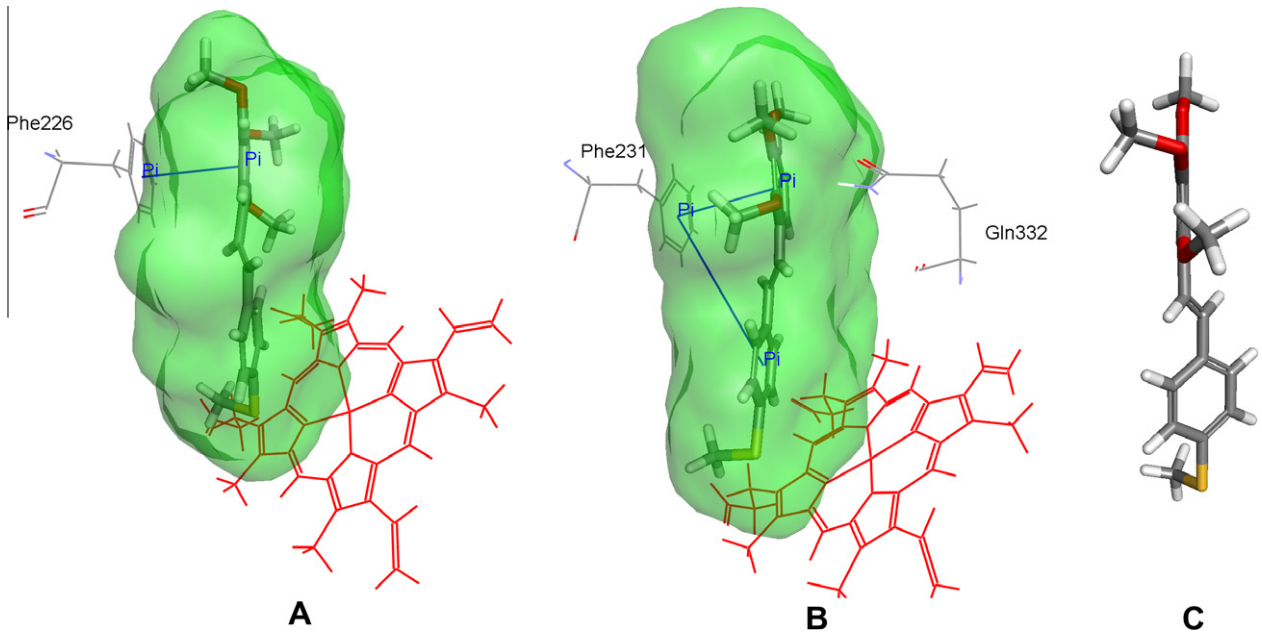

Figure 5. Comparison of the best poses of 2,3,4-trimethoxy-4′-methylthio-*trans*-stilbene (**S3**) in (A) CYP1A2 and (B) CYP1B1 binding cavities and (C) minimized structure of **S3**. Solid blue lines represent π–π interactions. Heme is represented as a wireframe model in red.

would help in the design of molecule(s) with desirable properties for future studies.

4. Experimental

4.1. Chemicals

Supersomes, microsomes from baculovirus-infected insect cells coexpressing NADPH-CYP reductase and CYP1A1, CYP1A2 or CYP1B1, were purchased from GENTEST (Woburn, MA, USA). The total CYP content was provided by the supplier. Glucose-6-phosphate dehydrogenase, nicotinamide adenine dinucleotide phosphate ($NADP^+$), 7-ethoxyresorufin and resorufin were obtained from Sigma (St. Louis, MO, USA). All the other chemicals and reagents were of the highest grade available. Reactions which involved air or moisture sensitive reagents were performed in oven-dried glassware under an argon atmosphere, unless otherwise stated. Before use, solvents for chromatography and isolation (ethyl acetate, hexanes) were purified by distillation. 4-methylthiobenzyl alcohol, methoxylated benzaldehydes and 2-chlorobenzaldehyde and other reagents and anhydrous solvents used in synthesis were generally purchased from Aldrich Chemical Company. All reaction mixtures were magnetically stirred and monitored by TLC.

NMR spectra for intermediates were recorded on a Varian Gemini 300 MHz model spectrometer (300 MHz for ^1H and 75 MHz for ^{13}C) and NMR spectra for final products were recorded on Bruker Avance II 400 (400 MHz for ^1H and 101 MHz for ^{13}C) with TMS as an internal standard in $CDCl_3$ unless otherwise specified. Chemical shifts are expressed in ppm (δ), and peaks are listed as singlet (s), doublet (d), triplet (t), quintet (q), multiplet (m), with coupling constants (J) expressed in Hertz. Melting points were determined in capillary tubes on a Stuart SMP10 micro melting point apparatus and are uncorrected. The LRMS (EI) spectra were recorded on Bruker 320MS/420GC mass spectrometer and HRMS (ESI) spectra were recorded on a Intectra Mass AMD 402 or 604 mass spectrometer. TLC was run on the silica gel coated plastic sheets (Silica Gel 60, 230–400 mesh, Merck, Germany) and visualized in UV light (254 or 365 nm).

4.2. Diethyl 4-(methylthiobenzyl) phosphonate (2)

4.2.1. 4-Methylthiobenzyl chloride (1)

To a solution of 4-methylthiobenzyl alcohol (13.0 g, 84.2 mmol) in anhydrous toluene (150 mL) was added dropwise neat thionyl chloride (7.6 mL, 12.4 g, 104 mmol) at room temperature. The resultant pale yellow solution was stirred at room temperature for 30 min, and ice-cold brine (150 mL) was added. The organic phase was separated, washed with ice-cold brine (5 × 150 mL), dried over $MgSO_4$ and filtered. The solvent was evaporated under reduced pressure. The residue (14.0 g) was distilled in vacuum at 115 °C/2.5 mmHg to yield **1** (12.27 g, 84.3%) of viscous oil which crystallized easily in refrigerator. ^1H NMR (300 MHz, $CDCl_3$) ppm (δ): 7.20–7.35 (m, 4H), 4.56 (s, 2H), 2.49 (s, 3H). ^{13}C NMR (75 MHz, $CDCl_3$) ppm (δ): 139.3, 134.3, 129.2, 126.7, 46.1, 15.8.

4.2.2. Diethyl 4-(methylthiobenzyl) phosphonate (2)

To a triethyl phosphite (14.27 mL, 13.82 g, 83.2 mmol) which was heated at reflux, 4-methylthiobenzyl chloride (12.27 g, 71.06 mmol) was added dropwise with stirring, at such a rate that a gentle reflux was maintained. When the addition was completed, the reaction was refluxed for an additional 2 h. The mixture was cooled to 25 °C, and the product mixture was fractionally distilled under vacuum to yield 15.6 g (80%) of water clear, viscous liquid: bp 142–145 °C/0.025 mmHg; ^1H NMR (300 MHz, $CDCl_3$) ppm (δ): 1.27 (t, J = 7.2, 6H), 2.49 (s, 3H), 3.13 (d, J = 21.6, 3H), 4.04 (q, J = 7.6, 4H); 7.23 (s, 4H).

4.3. General method of synthesis of compounds 4′-methylthiostilbene derivatives

A solution of **2** (1.5 g, 5.47 mmol) in dry DMF (10 mL) was added to a magnetically stirred solution of NaH (60% dispersion in mineral oil, 0.22 g, 5.47 mmol) in dry DMF under nitrogen (10 mL) at 0 °C, and the solution was stirred for 30 min. A solution of corresponding benzaldehyde (4.56 mmol) in dry DMF (10 mL) were added at 0 °C, and the reaction mixture was allowed to warm to room temperature over a period of 1.5 h. The mixture was poured slowly onto 250 mL ice-water and the precipitated solid was filtered, washed with water, dried, and crystallized from diluted or pure ethanol to yield white crystals.

4.3.1. 2,4-Dimethoxy-4′-methylthio-*trans*-stilbene (S1)

Yield: 0.91 g (70%); mp 107–108 °C; ^1H NMR (400 MHz, $CDCl_3$) ppm (δ): 7.51 (d, J = 8.50, 1H, C6-*H*), 7.45 (d, J = 8.40, 2H, C2′-*H*, C6′-*H*), 7.37 (d, J = 16.50, 1H, Cvin-*H*), 7.24 (d, J = 8.40, 2H, C3′-*H*, C5′-*H*), 6.98 (d, J = 16.50, 1H, Cvin′-*H*), 6.53 (d, J = 8.5, 1H, C5-*H*), 6.49 (s, 1H, C3-*H*), 3.89 (s, 3H, C4-OCH_3), 3.85 (s, 3H, C2-OCH_3), 2.51 (s, 3H, C4′-SCH_3).

^{13}C NMR (101 MHz, $CDCl_3$) ppm (δ): 160.46 (**C2**), 157.96 (**C4**), 136.76 (**C4′**), 135.41 (**C1′**), 127.12 (**C6**), 126.82 (**Cvin**), 126.66 (**C2′**, **C6′**), 126.30 (**C3′**, **C5′**), 122.72 (**Cvin′**), 119.48 (**C1**), 104.97 (**C5**), 98.46 (**C3**), 55.37 (C4-OCH_3), 55.37 (C2-OCH_3), 15.99 (C4′-SCH_3). LRMS (EI) m/z 286 [M^+, 100%]. HRMS (ESI) m/z Calcd for $C_{17}H_{18}O_2S$ $[M+H]^+$: 286.1028. Found: 286.1010.

4.3.2. 2,5-Dimethoxy-4′-methylthio-*trans*-stilbene (S2)

Yield: 0.85 g (65%); mp 58–60 °C; ^1H NMR (400 MHz, $CDCl_3$) ppm (δ): 7.47 (d, J = 8.30, 2H, C2′-*H*, C6′-*H*), 7.43 (d, J = 16.50, 1H, Cvin-*H*), 7.25 (d, J = 8.40, 2H, C3′-*H*, C5′-*H*), 7.16 (s, 1H, C6-*H*), 7.06 (d, J = 16.37, 1H, Cvin′-*H*), 6.85 (d, J = 8.9, 1H, C3-*H*), 6.81 (d, J = 8.9, 1H, C4-*H*), 3.86 (s, 3H, C2-OCH_3), 3.83 (s, 3H, C5-OCH_3), 2.51 (s, 3H, C4′-SCH_3).

^{13}C NMR (101 MHz, $CDCl_3$) ppm (δ):153.73 (**C2**), 151.38 (**C5**), 137.55 (**C4′**), 134.76 (**C1′**), 128.64 (**Cvin**), 127.20 (**C2′**, **C6′**), 126.96 (**C1**), 126.65 (**Cvin′**), 122.64 (**C3′**, **C5′**), 113.62 (**C4**), 112.25 (**C6**), 111.51 (**C3**), 56.22 (C2-OCH_3), 55.74 (C5-OCH_3), 15.81 (C4′-SCH_3). LRMS (EI) m/z 286 [M^+, 100%]. HRMS (ESI) m/z Calcd for $C_{17}H_{18}O_2S$ $[M+H]^+$: 286.1028. Found: 286.1030.

4.3.3. 2,3,4-Trimethoxy-4′-methylthio-*trans*-stilbene (S3)

Yield: 0.87 g (60%); mp 144–146 °C; ^1H NMR (400 MHz, $CDCl_3$) ppm (δ): 7.44 (d, J = 8.30, 2H, C2′-*H*, C6′-*H*), 7.30 (d, J = 16.30, 1H, Cvin-*H*), 7.30 (d, J = 8.8, 1H, C6-*H*), 7.24 (d, J = 8.30, 2H, C3′-*H*, C5′-*H*), 6.99 (d, J = 16.50, 1H, Cvin′-*H*), 6.70 (d, J = 8.8, 1H, C5-*H*), 3.91 (s, 3H, C3-OCH_3), 3.91 (s, 3H, C4-OCH_3), 3.88 (s, 3H, C2-OCH_3), 2.50 (s, 3H, C4′-SCH_3).

^{13}C NMR (101 MHz, $CDCl_3$) ppm (δ): 153.17 (**C2**), 151.64 (**C4**), 142.38 (**C3**), 137.26 (**C4′**), 134.93 (**C1′**), 127.21 (**C2′**, **C6′**), 126.72 (**Cvin**), 126.71 (**C3′**, **C5′**), 124.42 (**Cvin′**), 122.31 (**C6**), 120.56 (**C1**), 107.76 (**C5**), 61.26 (C3-OCH_3), 60.85 (C2-OCH_3), 55.99 (C4-OCH_3), 15.85 (C4′-SCH_3). LRMS (EI) m/z 316 [M^+, 100%]. HRMS (ESI) m/z Calcd for $C_{18}H_{12}O_3S$ $[M+H]^+$: 316.1133. Found: 316.1135.

4.3.4. 2,4,5-Trimethoxy-4′-methylthio-*trans*-stilbene (S4)

Yield: 0.91 g (63%); mp 113–115 °C; ^1H NMR (400 MHz, $CDCl_3$) ppm (δ): 7.46 (d, J = 8.30, 2H, C2′-*H*, C6′-*H*), 7.40 (d, J = 16.50, 1H, Cvin-*H*), 7.24 (d, J = 8.40, 2H, C3′-H, C5′-*H*), 7.13 (s, 1H, C6-*H*), 6.94 (d, J = 16.40, 1H, Cvin′-*H*), 6.55 (s, 1H, C3-*H*), 3.93 (s, 6H, C4-OCH_3, C5-OCH_3), 3.88 (s, 3H, C2-OCH_3), 2.51 (s, 3H, C4′-SCH_3).

^{13}C NMR (101 MHz, $CDCl_3$) ppm (δ): 151.68 (**C2**), 149.59 (**C4**), 143.44 (**C5**), 136.93 (**C4′**), 135.19 (**C1′**), 126.79 (**C2′**, **C6′**), 126.67 (**C3′**, **C5**), 126.16 (**Cvin**), 122.41 (**Cvin′**), 118.24 (**C1**), 109.34 (**C6**), 97.71 (**C3**), 56.68 (C4-OCH_3), 56.53 (C5-OCH_3), 56.06 (C2-OCH_3), 15.93 (C4′-SCH_3). LRMS (EI) *m/z* 316 [M$^+$, 100%]. HRMS (ESI) *m/z* Calcd for $C_{18}H_{12}O_3S$ [M+H]$^+$: 316.1133. Found: 316.1146.

4.3.5. 2,4,6-Trimethoxy-4′-methylthio-*trans*-stilbene (S5)

Yield: 0.69 g (48%); mp 109–110 °C; ^{1}H NMR (400 MHz, $CDCl_3$) ppm (δ): 7.49 – 7.41 (m, 3H, C2′-*H*, C6′-*H*, Cvin-*H*), 7.38 (d, *J* = 16.60, 1H, Cvin′-*H*), 7.24 (d, *J* = 8.50, 2H, C3′-*H*, C5′-*H*), 6.19 (s, 2H, C3-*H*, C5-*H*), 3.90 (s, 6H, C2-OCH_3, C6-OCH_3), 3.86 (s, 3H, C4-OCH_3), 2.51 (s, 3H, C4′-SCH_3).

^{13}C NMR (101 MHz, $CDCl_3$) ppm (δ): 160.17 (**C4**), 159.45 (**C2**, **C6**), 136.90 (**C4′**), 136.07 (**C1′**), 129.18 (**Cvin**), 126.93 (**C2′**, **C6′**), 126.55 (**C3′**, **C5′**), 119.37 (**Cvin′**), 108.10 (**C1**), 90.79 (**C3**, **C5**), 55.75 (C2-OCH_3, C6-OCH_3), 55.29 (C4-OCH_3), 16.16 (C4′-SCH_3). LRMS (EI) *m/z* 316 [M$^+$, 100%]. HRMS (ESI) *m/z* Calcd for $C_{18}H_{12}O_3S$ [M+H]$^+$: 316.1133. Found: 316.1146.

4.3.6. 3,4,5-Trimethoxy-4′-methylthio-*trans*-stilbene (S6)

Yield: 1.08 g (75%); mp 111–113 °C [lit. 109–111 °C[8]]; ^{1}H NMR (400 MHz, $CDCl_3$) ppm (δ): 7.22 (d, *J* = 8.30, 2H, C2′-*H*, C6′-*H*), 7.14 (d, *J* = 8.30, 2H, C3′-H, C5′-*H*), 6.51 (d, *J* = 16.50, 1H, Cvin-*H*), 6.48 (d, *J* = 16.30, 1H, Cvin′-*H*), 6.48 (s, 2H, C2-*H*, C6-*H*), 3.84 (s, 3H, C4-OCH_3), 3.68 (s, 6H, C3-OCH_3, C5-OCH_3), 2.46 (s, 3H, C4′-SCH_3).

^{13}C NMR (101 MHz, $CDCl_3$) ppm (δ): 152. 91 (**C3**, **C5**), 137.36 (**C4**), 137.21 (**C4′**), 134.04 (**C1′**), 132.55 (**C1**), 129.88 (**Cvin**), 129.41 (**C2′**, **C6′**), 129.28 (**Cvin′**), 126.16 (**C3′**, **C5′**), 105.94 (**C2**, **C6**), 60.90 (C4-OCH_3), 55.89 (C3-OCH_3, C5-OCH_3), 15.74 (C4′-SCH_3). LRMS (EI) *m/z* 301 (70), 316 [M$^+$, 100%]. HRMS (ESI) *m/z* Calcd for $C_{18}H_{12}O_3S$ [M+H]$^+$: 316.1133. Found: 316.1139.

4.3.7. 2-Chloro-4′-methylthio-*trans*-stilbene (S7)

Yield: 0.87 g (73%); mp 90–92 °C; ^{1}H NMR (400 MHz, $CDCl_3$) ppm (δ): 7.68 (d, *J* = 7.80, 1H, C6-*H*), 7.48 (d, *J* = 16.20, 1H, Cvin-*H*), 7.48 (d, *J* = 8.40, 2H, C2′-*H*, C6′-*H*), 7.39 (d, *J* = 7.90, 1H, C3-*H*), 7.26 (t, *J* = 6.30, 1H, C5-*H*), 7.26 (d, *J* = 8.50, 2H, C3′-*H*, C5′-*H*), 7.19 (t, *J* = 7.60, 1H, C4-*H*), 7.04 (d, *J* = 16.20, 1H, Cvin′-*H*), 2.51 (s, 3H, C4′-SCH_3).

^{13}C NMR (101 MHz, $CDCl_3$) ppm (δ): 138.50 (**C4′**), 135.38 (**C1′**), 133.95 (**C1**), 133.33 (**C2**), 130.56 (**C2′**, **C6′**), 129.81 (**C3**), 128.41 (**C4**), 127.18 (**Cvin**), 126.88 (**C6**), 126.58 (**C5**), 126.32 (**C3′**, **C5′**), 124.03 (**Cvin′**), 15.70 (C4′-SCH_3). LRMS (EI) *m/z* 178 (100), 260 [M$^+$, 93%]. HRMS (ESI) *m/z* Calcd for $C_{15}H_{13}ClS$ [M+H]$^+$: 260.4948. Found: 260.4936.

4.4. 7-Ethoxyresorufin *O*-deethylation (EROD) enzyme assay

To assess CYP1 enzyme activities 7-ethoxyresorufin *O*-deethylase (EROD) activity was measured according to the method of Burke et al.[38] The test compounds were freshly dissolved in dimethylsulfoxide (DMSO) on the day of experiment.

The reaction mixture (1 ml total volume) contained the various concentrations of a test compound, 1.3 mM NADP$^+$, 3.3 mM glucose-6-phosphate, 0.5 U/ml glucose-6-phosphate dehydrogenase, 3.3 mM magnesium chloride and 2 μM 7-ethoxyresorufin in 100 mM potassium phosphate (pH 7.4). The reactions were initiated by the addition of human recombinant cytochromes (1.25 pmole CYP1A1, 5 pmole CYP1A2 or 5 pmole CYP1B1) and samples were incubated at 37 °C for 15 min. The fluorescence of the product was determined on a HITACHI Model F 2500 fluorescence spectrophotometer (λ_{ex}550 and λ_{em}585). The quantitation of the deethylated metabolite was based on comparison of its fluorescence with resorufin as a standard. Control incubations did not contain the test compounds.

The concentrations of compounds required for 50% inhibition of catalytic activities (IC_{50}) were determined graphically by plotting percent of control enzyme activity versus inhibitor concentration. All assays were performed in three parallel experiments. The coefficient of variation did not exceed 15%.

4.5. NADPH oxidation

To establish whether 4′-methylthiostilbene derivatives are metabolized by CYP1A2, NADPH oxidation was estimated spectrophotometrically at 340 nm in the presence of enzyme according to the procedure described by Dávila-Borja et al. with minor modification.[39] Reaction mixture contained 5 pmol/ml CYP1A2 in Tris buffer, pH 7.4, and a stilbene derivative at the concentration in the range 1–50 μM. The reaction was initiated by adding of 0.2 mM NADPH. Incubation at 37 °C was carried on for 3 min and NADPH oxidation was spectrophotometrically recorded every 15 s. The amount of NADPH oxidized was calculated by using the extinction coefficient 6.22 [mM^{-1} cm^{-1}] at 340 nm. As a positive control, 7-ethoxyresorufin was used; at the concentration of 2 μM increase in NADPH oxidation was observed in the full range of time (3 min).

4.6. CYP1A2 metabolism

Reaction mixture containing 40 pmol human recombinant CYP1A2, 1.3 mM NADP, 3.3 mM glucose-6-phosphate, 1.5 U/ml glucose-6-phosphate dehydrogenase and 20 μM stilbene derivative: 3,4,5-trimethoxy-4′-methylthiostilbene or 2,4,5-trimethoxy-4′-methylthiostilbene as a substrate, was incubated at 37 °C for 30 min.

4.7. GC–MS analysis of metabolic products of 3,4,5-trimethoxy-4′-MTS and 2,4,5-trimethoxy-4′-MTS

Reference chromatograms and mass spectra of neat samples (50 μg/ml ethyl acetate) of **S6** and **S4** were obtained by GC–MS (Figs. 1 and 2, respectively). For the determination of metabolic products, 3 mg of lyophilized reaction solution was re-dissolved in 200 μl of distilled water then partitioned with ethyl acetate (100 μl, twice). The ethyl acetate layers were combined and dried under a stream of nitrogen, reconstituted to 50 μl of ethyl acetate, and used for GC–MS analysis. GC–MS was performed on a JEOL gcmate II Instrument (JEOL USA Inc., Peabody, MA) using a J&W DB-5 capillary column (0.25 mm internal diameter, 0.25 μM film thickness, and 30 m length; Agilent Technologies, Foster City, CA). The GC was run under the following temperature program: initial 250 °C held for 1 min, increased to 275 at 10 °C/min rate, increased to 300 °C at the rate of 3 °C/min and held at this temperature for 3.0 min. The carrier gas was ultrahigh purity helium, at 1 ml/min flow rate. The injection port, GC–MS interface and ionization chamber were at 250, 230, and 230 °C, respectively. The volume of injection was 1 μl, splitless injection. Mass spectra were acquired in positive electron impact (70 ev), low-resolution mode. Under these conditions **S6** had a retention time of 11.58 min (Fig. 1A) and **S4** had a retention time of 11.92 min (Fig. 2A). The monohydroxylated products were revealed from a reconstructed ion chromatogram specifying m/z 332 (Figs. 1C and 2C). Using *m/z* 348, no peak appeared indicating absence of dihydroxylated metabolites. GC–MS analyses were done in duplicates.

4.8. Docking

Analyzed molecules were docked to the active sites of CYP1A2 (PDB: 2HI4) and CYP1B1 (PDB: 3PM0) with the use of Accelrys Discovery Studio 2.5.5 suite of programs by LigandFit procedure.[40] For

these two targets all water molecules were removed and hydrogen atoms were added. While coordinates of all heavy atoms were kept frozen, hydrogen atoms positions were optimized with the use of adopted basis Newton-Raphson minimization algorithm (max steps = 500, RMS gradient = 0.01 and distance-dependent dielectrics as implicit solvent model). The binding site was defined from the volume of a cocrystallized ligand (α-naphthoflavone). The grid resolution was set to default value of 0.5 Å.

For the conformational search of the ligands a Monte Carlo method was employed. During this search internal ligand electrostatic energy was not included and the variable number of trials, depending on the number of rotatable ligand bonds, was used according to non-modified default settings for LigandFit procedure. In all calculations for proteins and ligands CHARMm forcefield with MMFF94 partial charge rules were used. For docking we have used default values of parameters, except for DockScore function, where CFF force field was used instead of default Dreiding.

Twenty poses were saved for each ligand after docking and then minimized in situ with use of adopted basis Newton-Raphson algorithm. During each docking run poses were scored with seven scoring functions DockScore (CFF), LigScore1, LigScore2, PLP1, PLP2, Jain and PMF (Table S1–S3). For further evaluation DockScore CFF function (DockScore CFF force field version) was chosen as exhibiting the best correlation with experimental data. CFF force field was used also for LigScore calculations. For saved poses we applied protocol 'Analyze ligand poses' to calculate RMS deviation using first pose of each ligand as a reference and to find hydrogen bonds and close contacts. After visual inspection of poses and analysis of RMSD values, repeated poses were discarded. For the best poses, these characterized by the highest values of DockScore function, molecular volume and strain energy were calculated.

Acknowledgment

This work was supported by funding from Poznań University of Medical Sciences (Grant No 501-01-03313427-08032).

Supplementary data

Supplementary data associated with this article can be found, in the online version, at http://dx.doi.org/10.1016/j.bmc.2012.07.012.

References and notes

1. Goswami, S. K.; Das, D. K. *Cancer Lett.* **2009**, *284*, 1.
2. Rimando, A.; Suh, N. *Planta Med.* **2008**, *74*, 1635.
3. Bishayee, A.; Politis, T.; Darvesh, A. S. *Cancer Treat. Rev.* **2010**, *36*, 43.
4. Kundu, J.; Surh, Y.-J. *Cancer Lett.* **2008**, *269*, 243.
5. Saiko, P.; Szakmary, A.; Jaeger, W.; Szekeres, T. *Mutat. Res.* **2008**, *658*, 68.
6. Lappano, R.; Rosano, C.; Madeo, A.; Albanio, L.; Plastina, P.; Gabriele, B.; Forti, L.; Stivala, L. A.; Iacopetta, D.; Dolce, V.; Andò, S.; Pezzi, V.; Maggiolini, M. *Mol. Nutr. Food Res.* **2009**, *53*, 845.
7. Kang, S. S.; Cuendet, M.; Endringer, D. C.; Croy, V. L.; Pezzuto, J. M.; Lipton, M. A. *Bioorg. Med. Chem.* **2009**, *17*, 1044.
8. Cushman, M.; Nagarathnam, D.; Gopal, D.; He, H.-M.; Lin, C. M.; Hamel, E. *J. Med. Chem.* **1992**, *35*, 2293.
9. Ma, Z.; Molavi, O.; Haddadi, A.; Lai, R.; Gossage, R. A.; Lavasanifar, A. *Cancer Chemother. Pharmacol.* **2008**, *63*, 27.
10. Mazué, F.; Colin, D.; Gobbo, J.; Wegner, M.; Rescifina, A.; Spatafora, C.; Fasseur, D.; Delmas, D.; Meunier, P.; Tringali, C.; Latruffe, N. *Eur. J. Med. Chem.* **2010**, *45*, 2972.
11. Walle, T.; Hsieh, F.; DeLegge, M. H.; Oatis, J. E., Jr.; Walle, U. K. *Drug Metab. Dispos.* **2004**, *32*, 1377.
12. Walle, T.; Ta, N.; Kawamori, T.; Wen, X.; Tsuji, P. A.; Walle, U. K. *Biochem. Pharmacol.* **2007**, *73*, 1288.
13. Wilson, M. A.; Rimando, A. M.; Wolkow, C. A. *BMC Pharmacol.* **2008**, *8*, 15.
14. Liehr, J. G.; Ricci, M. J. *Proc. Natl. Acad. Sci. U.S.A.* **1996**, *93*, 3294.
15. Bruno, R. D.; Njar, V. C. O. *Bioorg. Med. Chem.* **2007**, *15*, 5047.
16. Jennings, B. L.; Sahan-Firat, S.; Estes, A. M.; Das, K.; Farjana, N.; Fang, X. R.; Gonzales, F. J.; Malik, K. U. *Hypertension* **2010**, *56*, 667.
17. Chang, T. K. H.; Chen, J.; Lee, W. B. K. *JPET* **2001**, *299*, 874.
18. Guengerich, F. P.; Chun, Y.-J.; Kim, D.; Gillam, E. M. J.; Shimada, T. *Mutat. Res.* **2003**, *523–524*, 173.
19. Mikstacka, R.; Rimando, A. M.; Szalaty, K.; Stasik, K.; Baer-Dubowska, W. *Xenobiotica* **2006**, *36*, 269.
20. Mikstacka, R.; Przybylska, D.; Rimando, A. M.; Baer-Dubowska, W. *Mol. Nutr. Food Res.* **2007**, *51*, 517.
21. Chun, Y. J.; Kim, S.; Kim, D.; Lee, S. K.; Guengerich, F. P. *Cancer Res.* **2001**, *61*, 8164.
22. Chun, Y. J.; Lim, C.; Ohk, S. O.; Lee, J. M.; Lee, J. H.; Choi, S.; Kim, S. *Med. Chem. Commun.* **2011**, *2*, 402.
23. Chun, Y. J.; Ryu, S. Y.; Leong, T. C.; Kim, M. Y. *Drug Metab. Dispos.* **2001**, *29*, 389.
24. Mikstacka, R.; Baer-Dubowska, W.; Wieczorek, M.; Sobiak, S. *Mol. Nutr. Food Res.* **2008**, *52*, S77.
25. Yang, H.; Baur, J. A.; Chen, A.; Miller, C.; Sinclair, D. A. *Aging Cell* **2007**, *6*, 35.
26. Vasanthanathan, P.; Hritz, J.; Taboureau, O.; Olsen, L.; Jorgensen, F. S.; Vermeulen, N. P. E.; Oostenbrink, C. *J. Chem. Inf. Model.* **2009**, *49*, 43.
27. Smith, D. A.; Ackland, M. J.; Jones, B. C. *Drug Discov. Today* **1997**, *2*, 406.
28. Don, M.-J.; Lewis, D. F. V.; Wang, S.-Y.; Tsai, M.-W. *Bioorg. Med. Chem. Lett.* **2003**, *13*, 2535.
29. Lewis, D. F. V.; Lake, B. G.; Dickins, M. *Xenobiotica* **2004**, *34*, 501.
30. Lewis, D. F. V.; Ito, Y.; Lake, B. G. *Toxicol. In Vitro* **2006**, *20*, 256.
31. Takemura, H.; Itoh, T.; Yamamoto, K.; Sakakibara, H.; Shimoi, K. *Bioorg. Med. Chem.* **2010**, *18*, 6310.
32. Piver, B.; Fer, M.; Vitrac, X.; Merillon, J.-M.; Dreano, Y.; Berthou, F.; Lucas, D. *Biochem. Pharmacol.* **2004**, *68*, 773.
33. Sansen, S.; Yano, J. K.; Reynald, R. L.; Schoch, G. A.; Griffin, K. J.; Stout, C. D.; Johnson, E. F. *J. Biol. Chem.* **2007**, *282*, 14348.
34. Wang, A.; Savas, U.; Stout, C. D.; Johnson, E. F. *J. Biol. Chem.* **2011**, *286*, 5736.
35. Montes, M.; Miteva, M. A.; Villoutreix, B. O. *Proteins* **2007**, *68*, 712.
36. Li, X.; Li, Y.; Cheng, T.; Liu, Z.; Wang, R. *J. Comp. Chem.* **2010**, *31*, 2109.
37. de Graaf, C.; Oostenbrink, C.; Keizers, P. H.; van der Wijst, W. T.; Jongejan, A.; Vermeulen, N. P. E. *J. Med. Chem.* **2006**, *49*, 2417.
38. Burke, M. D.; Thompson, S.; Elcombe, C. R.; Halpert, J.; Haaparanta, T.; Mayer, R. T. *Biochem. Pharmacol.* **1985**, *34*, 3337.
39. Dávila-Borja, V. M.; Belmont, J. A.; Espinosa, J. J.; Moreno-Sanchez, R.; Albores, A.; Montero, R. D. *Arch. Toxicol.* **2007**, *81*, 697.
40. Venkatachalam, C. M.; Jiang, X.; Oldfield, T.; Waldman, M. *J. Mol. Graph. Model.* **2003**, *21*, 289.